



ELSEVIER

Available online at www.sciencedirect.com

SCIENCE @ DIRECT®

Journal of Sound and Vibration 285 (2005) 251–265

JOURNAL OF
SOUND AND
VIBRATION

www.elsevier.com/locate/jsvi

Wave component analysis of energy flow in complex structures – Part III: two coupled plates

E.C.N. Wester^{a,*}, B.R. Mace^b

^a*Industrial Research Limited, P.O. Box 2225, Auckland, New Zealand*

^b*ISVR, University of Southampton, Highfield, Southampton SO17 1BJ, UK*

Received 30 January 2004; received in revised form 18 August 2004; accepted 19 August 2004

Available online 22 December 2004

Abstract

A statistical, wave-based approach to the analysis of energy flow in structures is applied to example structures comprising two, regularly or irregularly coupled, rectangular plates. The approach, which is developed in two companion papers, is based on the expression of the response in terms of energy-bearing ‘wave components’ and a description of the structure in terms of subsystem and junction wave component scattering matrices, **S** and **T**. Uncertainty in the properties of the structure is taken into account by assuming that the structure is drawn from an ensemble of structures which vary randomly in detail. A ‘scalar random phase’ ensemble is defined in terms of a random distribution of the eigenvalues of the global scattering matrix product **ST**. Analytical expressions enable the ensemble mean and variance of energy responses over this ensemble to be found at low computational cost. Scalar random phase ensemble-based estimates of these statistics for regularly and irregularly coupled plate structures are found to be in good agreement with the results of Monte Carlo simulations.

© 2004 Elsevier Ltd. All rights reserved.

1. Introduction

Traditional dynamic modelling methods such as finite element analysis cannot generally be applied to ‘complex’ structures which involve high frequency excitation and significant modeling

*Corresponding author. Tel.: +64 9 920 3100; fax: +64 9 920 3116.

E-mail addresses: e.wester@irl.cri.nz (E.C.N. Wester), brm@isvr.soton.ac.uk (B.R. Mace).

uncertainty. For these, differences between the structure and its mathematical model lead to significant differences between the predicted and actual response, the high level of spatial detail assumed in the model is informationally unwarranted and the magnitude of the computational task is prohibitive. One method which attempts to address these difficulties is that known as statistical energy analysis (SEA) [1]. The validity of assumptions upon which SEA is based is often unclear, however, and there is wide interest in more rigorous approaches.

An alternative method, which avoids a number of assumptions of SEA, is applied in this paper to the analysis of two-plate structures. Its theoretical basis is described in two companion papers which deal, respectively, with a deterministic wave component model [2] and with its development into a statistical approach for complex structures [3].

In this approach, the response of the structure to external forcing is described in terms of energy-bearing ‘wave components’ which propagate through the structure and are reflected and transmitted at junctions and in subsystems. The relationships between the amplitudes of wave components at cross-sections of the structure are expressed in terms of global subsystem and junction scattering matrices \mathbf{S} and \mathbf{T} , which are systematically assembled from local reflection and transmission coefficients. The dynamic properties of the structure overall can then be described in terms of the matrix product \mathbf{ST} or, equivalently, in terms of the eigenvalues and eigenvectors of \mathbf{ST} .

Structural uncertainty is modelled by assuming that the structure at hand is drawn from an ensemble of structures which vary randomly in detail. Variations in structural properties over the ensemble then lead to changes in the matrix \mathbf{ST} and its spectral properties. It has been observed [3] that variations in the energy response of the structure are strongly associated with ‘common’ changes in the phases of the eigenvalues of \mathbf{ST} . A ‘scalar random phase’ (or ‘scalar’) ensemble is defined in terms of a uniform random distribution of this common eigenvalue phase, which is found to be a good approximation to many practical ensembles. Analytical expressions for the mean and variance of the energy response over this ensemble have been found, which allow estimates of these statistics to be found for practical ensembles at relatively low computational cost.

Two forms of coupled plate structure are considered in this paper. One of these is ‘regular’ and can be described in a separable coordinate system. Wave components then propagate as if confined to dynamically one-dimensional structures, between which there is no transfer of energy. This kind structure has been considered in detail by Wester and Mace [4]. The other structure is not regular in this sense and energy can pass more or less freely between wave components of different trace wavenumber.

Details of the two kinds of two-plate structures are given in the section that follows. In Section 3, an outline is presented of the procedures which are used to generate numerical ensembles of structures for comparing the characteristics of scalar and practical ensembles. In Section 4, underpinning assumptions concerning the ensemble variations of the eigenvalues and eigenvectors are investigated, together with the effect of structural regularity on these assumptions. The adequacy of the scalar ensemble in describing the statistical distributions of the energy responses expected in practical ensembles is examined in Section 5, and the accuracy of analytical expressions for the mean and variance of responses over the scalar ensemble is demonstrated by comparison with the results of Monte Carlo simulations.

2. Two-plate structure

The general form of the structures considered in this paper is illustrated in Fig. 1. A deterministic wave component model is described in Ref. [2] and will be repeated here in outline only.

Two uniform rectangular plates, with the nominal properties given in Table 1, are joined rigidly along a common edge. All the outside edges of the structure are simply supported, and out-of-plane motion along the coupling is constrained by a line translational spring of stiffness 10^8 N/m^2 , which extends over a part of the width of the plates. In-plane motion of the plates is neglected.

Flexural waves are generated in the structure by time-harmonic rain-on-the-roof forcing applied to plate A. The plates act as waveguides in which the flexural wave field can be described in terms of wave components obtained by Fourier decomposition over the y -coordinate. Since the plates are simply supported at the edges, this variation with y has the form

$$\Psi_i(y) = \sqrt{2/d} \sin(k_{yi}y), \quad i = 1, 2, \dots, \tag{1}$$

where d is the plate width and $k_{yi} = i\pi/d$ is a trace wavenumber that identifies each wave component. Apart from near-field components, which are ignored here, the total field is a superposition of positive- and negative-going wave components.

It is convenient to assemble the amplitudes of the two sets of components at any cross-section across the plates into column vectors. Global subsystem and junction scattering matrices **S** and **T**

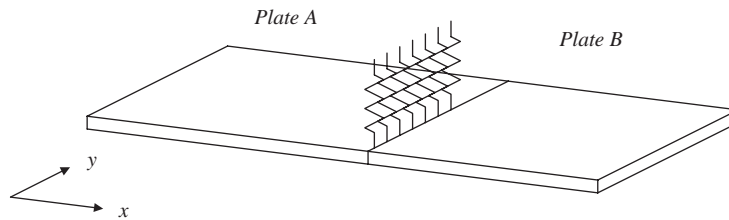


Fig. 1. Rectangular plate structure with line translational spring.

Table 1
Nominal plate properties

Property	Nominal value
Length, plate A	840 mm
Length, plate B	680 mm
Width	520 mm
Thickness	1.0 mm
Density	8000 kg/m ³
Young's modulus	$2 \times 10^{11} \text{ N/m}^2$
Poisson's ratio	0.3

can then be constructed, which quantify the changes in amplitudes of wave components as they undergo reflection and transmission at the cross-sections between the plates and junction. These are given, respectively, by

$$\mathbf{S} = \begin{bmatrix} \mathbf{S}_A & \mathbf{0} \\ \mathbf{0} & \mathbf{S}_B \end{bmatrix}, \quad \mathbf{T} = \begin{bmatrix} \mathbf{R}_A & \mathbf{T}_{AB} \\ \mathbf{T}_{AB}^T & \mathbf{R}_B \end{bmatrix}. \quad (2)$$

Here, \mathbf{S}_A and \mathbf{S}_B are matrices which describe local wave component reflection in each of the two plates and \mathbf{T}_{AB} , \mathbf{R}_A and \mathbf{R}_B are corresponding matrices which describe wave component transmission and reflection at the junction. (These are derived explicitly for this structure in Ref. [5].)

The wave component scattering properties of the junction depend on the length of the spring. If the spring spans the full width of the plates, the structure is completely regular and wave components are confined to dynamically one-dimensional waveguides between which there is no exchange of energy. All the local matrices \mathbf{S}_A , \mathbf{S}_B , \mathbf{T}_{AB} , \mathbf{R}_A and \mathbf{R}_B are then diagonal. If the spring spans only a part of the width of the plates, energy can be transferred between wave components of different trace wavenumber, and the local scattering matrices \mathbf{T}_{AB} , \mathbf{R}_A and \mathbf{R}_B may have significant off-diagonal entries.

Two kinds of structure will be considered in the following discussion, of which one is regular with a spring of length d and the other is irregular with a spring that spans 0.61 of the width. The structures are nominally the same in all other respects.

3. Ensembles of structures

Uncertainty concerning structural properties is accounted for by assuming that the structure at hand is one drawn from an ensemble of structures which have geometric and material properties that differ randomly in detail. These variations lead to a range of structural responses and, hence, to a range of each of the scattering matrices \mathbf{S} and \mathbf{T} . Two kinds of ensemble will be considered.

The first is a ‘Monte Carlo’ ensemble, which is taken to be representative of practical ensembles. In this ensemble, the properties of the plates are statistically independent random variables, normally distributed about the nominal values given in Table 1. In many practical cases, the statistical independence of uncertain properties is clear. In others, it is sometimes possible to transform dependent to independent properties.

Figs. 2 and 3 show the probability density functions of the energy flow between regularly and irregularly coupled plates for a range of coefficients of variation (standard deviation divided by the average). The frequency of excitation is 2000 Hz and the plate loss factor $\eta = 0.001$. At this frequency, the mode count is approximately 520 and the modal overlap factor $M = 0.52$. Each probability density function estimate involves 75 bins and is derived from 100,000 samples. In each case, the figures indicate that the dependence of the distribution on the assumed variance decreases rapidly as the coefficient of variation is increased from zero, and that the distribution is approximately constant for coefficients of variation greater than about 5%. It will be assumed in the discussion that follows that each property has a coefficient of variation of 5%.

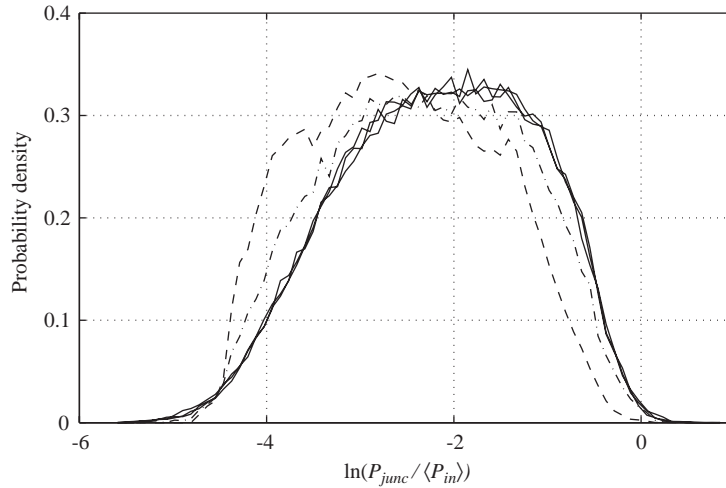


Fig. 2. Probability density function of the log of the normalised junction power for the *regular* plate structure and coefficients of variation 0.5% (- - - -), 1% (- · · · · ·), and 2%, 5% and 10% (—).

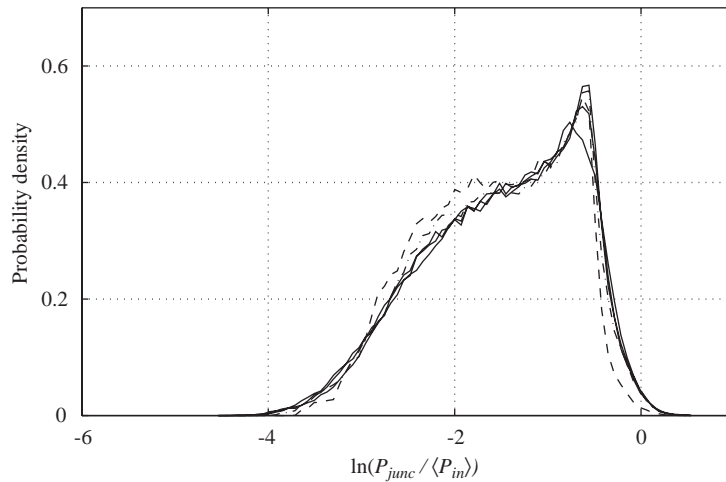


Fig. 3. Probability density function of the log of the normalised junction power for the *irregular* plate structure and coefficients of variation 0.5% (- - - -), 1% (- · · · · ·), and 2%, 5% and 10% (—).

The second ensemble that will be considered is the scalar random phase ensemble, defined in terms of the product \mathbf{ST} of the global scattering matrices. If $(\mathbf{ST})_0$ is this product for the structure at hand, members of the ensemble have corresponding products given by $e^{i\theta}(\mathbf{ST})_0$, where θ is a random variable uniformly distributed in $[-\pi, \pi]$. The magnitudes and relative phases of the entries of \mathbf{ST} are constant over this ensemble, as are the eigenvectors and the magnitudes of the eigenvalues. Variations in θ lead to a common change in phase in all the entries of \mathbf{ST} and all its eigenvalues.

4. Eigenvalues and eigenvectors

Although the statistical distribution of the responses of a structure with uncertainty can be expressed formally in terms of the joint probability density function of the uncertain properties, this is not practical in most applications. In this section, the example structures described in earlier sections are used to demonstrate the use of the scalar ensemble in deriving computationally inexpensive estimates of ensemble statistics. Justification is given for the use of the scalar ensemble by quantitative demonstration of observations made in Ref. [3] concerning ensemble variations of the eigenvalues and eigenvectors of **ST**. The variations of these spectral parameters over the Monte Carlo ensemble are considered for regular and irregular coupled-plate structures and the effect of structural regularity on the statistical distributions of the spectral parameters is investigated.

4.1. Eigenvalues

Examples of the variations of the magnitudes and phases of eigenvalues over the Monte Carlo ensemble are shown in Figs. 4 and 6 for regular and irregular structures, respectively. The excitation frequency is 100 Hz and the plate loss factor $\eta = 0.005$. At this frequency, the order of the global scattering matrices is 6 and the mode count is approximately 26.

The data shown in these figures have been obtained from 12 random points in the ensemble. A smooth path through the ensemble has been defined by interpolating the structural properties between pairs of random points and the figures show the continuous variation of the eigenvalues of **ST** over this path.

The regular structure, as noted earlier, can be described in dynamic terms as a number of one-dimensional waveguides. Each of these comprises two subsystems and is associated with a single trace wavenumber and an identifiable pair of eigenvalues. Pairs of associated eigenvalues can be identified in the upper part of Fig. 4 by the similarity in the trajectories of their magnitudes.

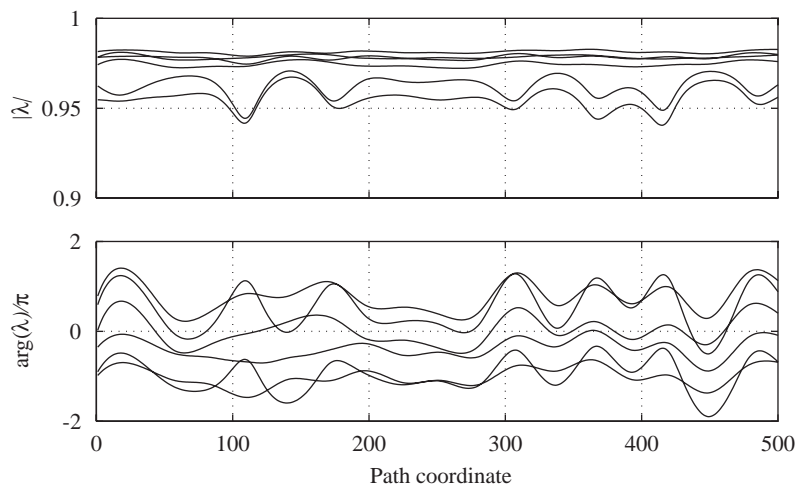


Fig. 4. Variation of eigenvalue magnitude and phase for a *regular* system over a path in the ensemble.

Each of the two eigenvalues associated with a given dynamically one-dimensional system or trace wavenumber repels its partner with a strength that depends only on the magnitude of the corresponding junction reflection coefficient [3]. There is no repulsion between eigenvalues associated with different trace wavenumbers. In terms of the phase trajectories shown in the lower part of Fig. 4, paths corresponding to eigenvalues associated with the same trace wavenumber never cross, while those corresponding to eigenvalues associated with different trace wavenumbers cross freely. These features are illustrated more clearly in Fig. 5, which shows the phases of the three pairs of the eigenvalues in separate graphs. The magnitude of the junction reflection coefficient is an increasing function of trace wavenumber and the strongest eigenvalue repulsion occurs between the pairs shown in the upper graph. The repulsion is weakest between the pairs in the lowest graph, which occasionally approach each other relatively closely. This pair corresponds to those with the smallest magnitudes.

These figures also demonstrate that the sensitivity of the eigenvalues to structural variation is greatest when the separation between eigenvalues that repel is small. The magnitudes and phase separations of eigenvalues are most stable and vary least rapidly, on the other hand, when the eigenvalues are well separated. The weakly repelling pair of eigenvalues in Figs. 4 and 5 (which can approach each other most closely) show the greatest variations in magnitude and phase.

Irregularity in a structure introduces the potential for energy to flow between wave components of different trace wavenumber and for repulsion between all eigenvalues. This is indicated in Fig. 6, where no two eigenvalue phase trajectories cross. (Although trajectories occasionally pass each other very closely, apparent crossings in Fig. 6 can be revealed as such by further interpolation.) The more constant separation between the phases of eigenvalues, which is evident in Fig. 6, also demonstrates that ensemble variations in the eigenvalues of the irregular structure are well characterised by changes in the common component of phase.

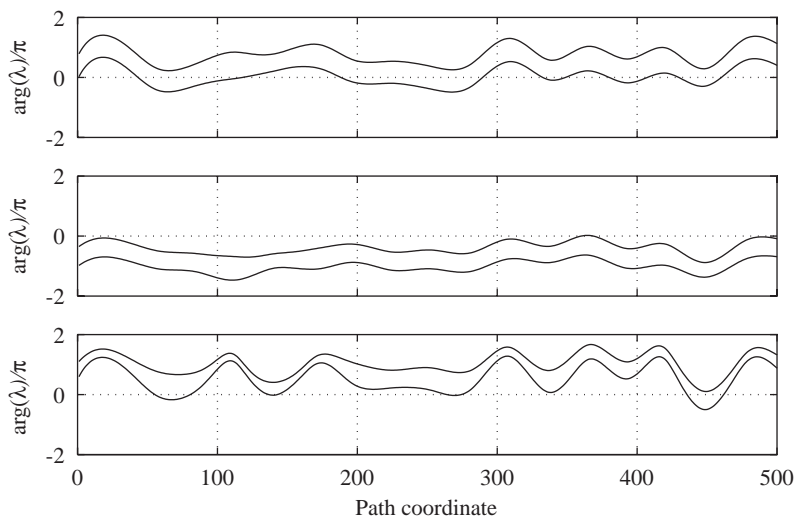


Fig. 5. Eigenvalue phases taken from Fig. 4 separated into pairs according to their association with a single trace wavenumber. Trace wavenumber increasing from bottom to top.

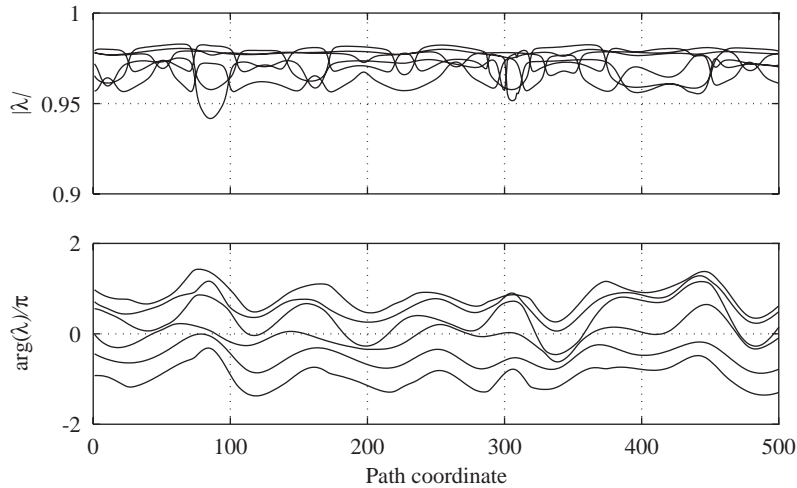


Fig. 6. Variation of eigenvalue magnitude and phase for an *irregular* system over a path in the ensemble.

Figs. 4–6 also illustrate the observations made in Ref. [3] concerning the relative insensitivity of the eigenvalue magnitudes to structural variations and the ‘common mode’ nature of the variations in phases of the eigenvalues (particularly for the irregular structure).

4.2. Distributions of eigenvalue phase spacing

Although ensemble variations in eigenvalue phase spacing do not play a central role in determining the energy response of the structure, a number of observations can be made concerning limiting cases which are of interest.

An estimate of the probability density function of the nearest-neighbour eigenvalue phase spacings for the regular structure is shown in Fig. 7. The frequency of excitation is 1000 Hz and $\eta = 0.005$. The estimate is based on 5000 samples of structures, each with 20 eigenvalues. The density function for the circular Poisson distribution [5], which corresponds to structures with no interaction between eigenvalues, is also shown in this figure and is very similar to the density for the regular structure. It has been found from simulations that the accuracy of fit between the two functions improves as the width of the plates and the number of eigenvalues increases. This can be attributed to the fact that the total number of interacting pairs of eigenvalues increases approximately as the square of the number of eigenvalues, while the number of potentially strong interactions (those associated with the same trace wavenumber) increases only linearly with this number. When the plates are wide and the number of wave components and eigenvalues is large, the interaction between eigenvalues is small on average.

An estimate of the probability density function for the irregular structure is shown in Fig. 8. The effects of stronger eigenvalue repulsion in this structure are clearly indicated by the very small probability that nearest eigenvalues have small phase spacing. The distribution lies between the extremes of no repulsion and strong repulsion, which have density functions corresponding to the

circular Poisson distribution or a delta function at $\phi/\phi_{avg} = 1$, respectively. The eigenvalue spacing distribution function for the circular unitary ensemble, which corresponds to all unitary matrices with the same order as **ST** [3], is also given for comparison.

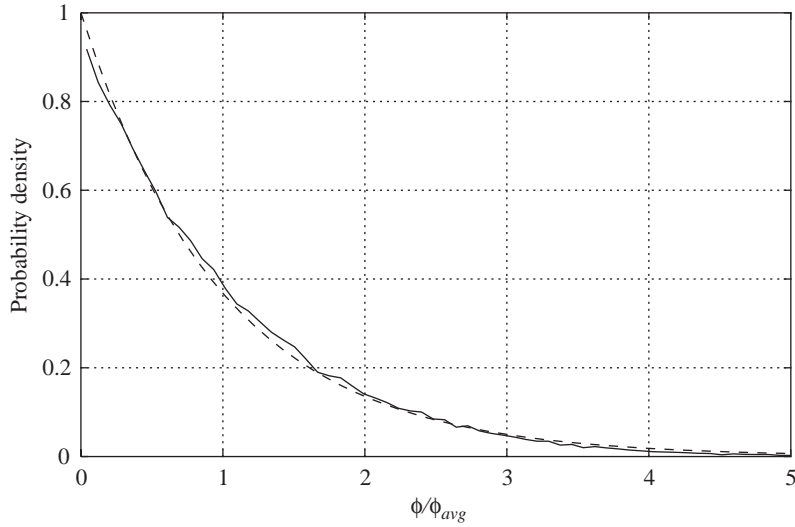


Fig. 7. Probability density function for nearest-neighbour spacings between eigenvalue phases for the *regular* plate system (—) and density function for the circular Poisson ensemble (- - -).

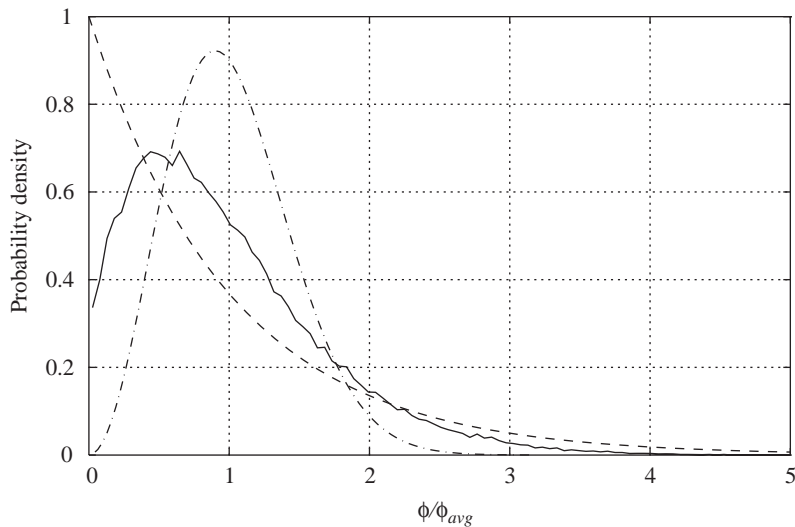


Fig. 8. Probability density function for nearest-neighbour spacings between eigenvalue phases for the *irregular* plate system (—). Density functions for the circular Poisson ensemble (- - -) and the circular unitary ensemble (- · - · -) are also shown.

Similar results have been found by Lyon and DeJong [1] for the natural frequencies of a simply supported rectangular plate and a similar plate which is clamped on one corner.

4.3. Eigenvectors

Qualitative features of the eigenvectors of the regular and irregular structures also differ. Examples from the ensemble of eigenvector matrices for each structure are shown in Fig. 9. At the excitation frequency of 2000 Hz, the structures have 30 eigenvalues. Eigenvectors appear as columns j in Fig. 9, and wave components in plate A correspond to entries i in the upper half of the matrices, while components in B correspond to those in the lower half.

As with the eigenvalues, the eigenvectors for the regular system can be grouped into pairs, where each pair is associated with a single trace wavenumber. The eigenvectors shown in Fig. 9(a) are sorted into pairs, with trace wavenumber increasing from left to right. It can be seen from this figure that one of the eigenvectors of each pair typically involves a large contribution corresponding to a wave component in plate A and a small contribution corresponding to a wave component with the same trace wavenumber in B. The converse is the case for the second of the pair. The degree of this localisation increases from left to right, with the trace wavenumber, because the magnitude of the transmission coefficient at the junction decreases with trace wavenumber.

Fig. 9(b) indicates that the eigenvectors of the irregular structure tend generally to be less localised and to involve contributions from wave components in both plates. Eigenvectors and one-dimensional waveguides and eigenvectors involve contributions from wave components with a number of different trace wavenumbers. An analogy can be drawn between the localisation of eigenvectors described here and the localisation of the normal modes of vibration which has been found to occur in two-plate structures. It has been shown in numerical simulations using finite element analysis that modes of uniform, rectangular plate structures tend to be more strongly localised in one or other of the plates than those in irregular structures [6].

For a structure comprising a pair of coupled one-dimensional subsystems A and B, a global subsystem matrix can be constructed in which the subsystem reflection coefficients s_A and s_B are

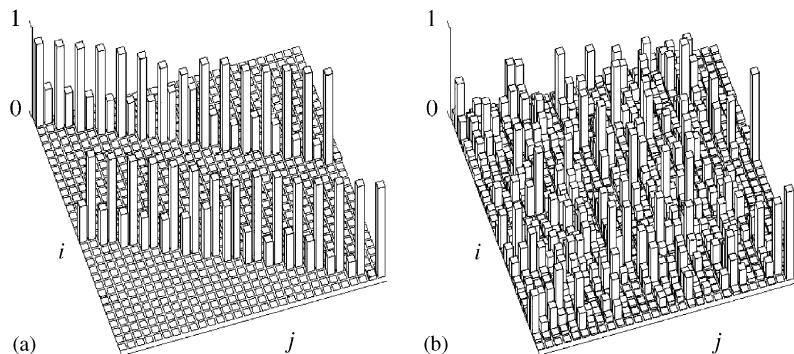


Fig. 9. Example eigenvector matrices for lightly damped ($\eta = 0.005$), regular (a) and irregular (b) plate structures. The entry (1, 1) is drawn in the upper left corner. Rows i correspond to wave components, with wave components in plate A in the upper half of the matrix, and columns j correspond to eigenvectors.

the diagonal entries. If $|s_A| = |s_B|$, the eigenvectors do not depend on the level of damping in the structure [3]. For one-dimensional subsystems with $|s_A| \neq |s_B|$, the eigenvectors show a small dependence on damping. It is then to be expected that the eigenvectors of regular two-plate structures, whose response can be described in terms of dynamically one-dimensional waveguides, are similarly approximately independent of damping.

5. Junction powers

The response of the structure to excitation can be described in terms of the power which flows through the junction between the plates or in terms of the plate energies which can be found from the input and junction powers. It is shown in this section that there is generally good agreement between the low-order moments of the probability density functions of the junction power for both the Monte Carlo and the scalar ensembles, and that this allows estimates of these quantities to be found at low computational cost.

5.1. Probability distributions

Figs. 10 and 11 show estimates of the ensemble probability distributions of the logarithm of the junction power in the regular and irregular plate structures for both the Monte Carlo and scalar ensembles. The distributions of powers in these structures are often highly non-normal. The junction power is normalised with respect to the ensemble-averaged input power and each probability density function estimate involves 75 bins and is derived from 100,000 samples. For each example, the frequency of excitation is 2000 Hz and $\eta = 0.001$.

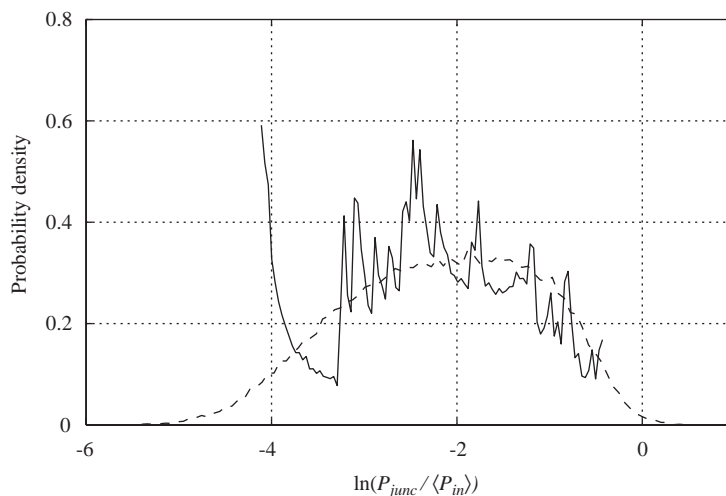


Fig. 10. Probability density function of the log of the normalised junction power for scalar (—) and Monte Carlo (---) ensembles for the *regular* plate structure.

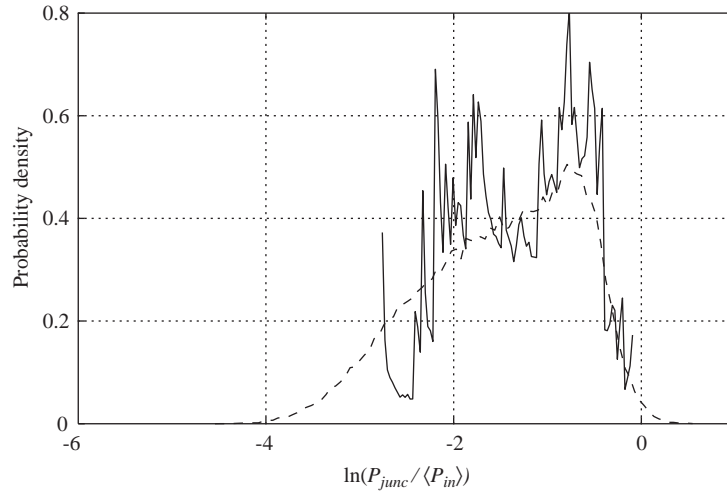


Fig. 11. Probability density function of the log of the normalised junction power for scalar (—) and Monte Carlo (---) ensembles for the *irregular* plate structure.

These figures suggest that the low-order moments of the Monte Carlo and scalar ensemble distributions are very similar and that differences between the ensembles are associated with higher-order moments. Analytical expressions for the mean and variance of the junction power over the scalar ensemble, which have been derived in Ref. [3], may therefore be expected to give good approximations to the mean and variance over the Monte Carlo ensemble.

It is also noted that the broader shape of the probability density function for the regular structure is associated with the generally weaker eigenvalue repulsion between eigenvalues in this structure. At any given frequency, very large junction powers occur in ensemble members which are resonant and have eigenvalues with phase close to zero. Conversely, very small junction powers occur in members which are non-resonant and have eigenvalues close to π . When the repulsion is weak, there is a greater probability that multiple ensemble members have eigenvalues close to one of these extremes [3].

5.2. Ensemble averages

Figs. 12 and 13 show estimates of the ensemble-averaged junction powers for the example regular and irregular structures as a function of the damping factor of the plate material. The estimates based on the scalar ensemble, obtained by direct evaluation of expressions given in the earlier reference, agree well with numerical estimates obtained from 50,000 samples of the Monte Carlo-generated ensemble. A more accurate scalar ensemble estimate is also shown, which corresponds to the average of results obtained by applying this same equation to 10 structures randomly selected from the Monte Carlo-generated ensemble. The accuracy of the scalar ensemble estimate is seen to be best for the case of the irregular structure in which eigenvalue repulsion is strong and variations in the ensemble are most accurately represented by changes in the common eigenvalue phase.

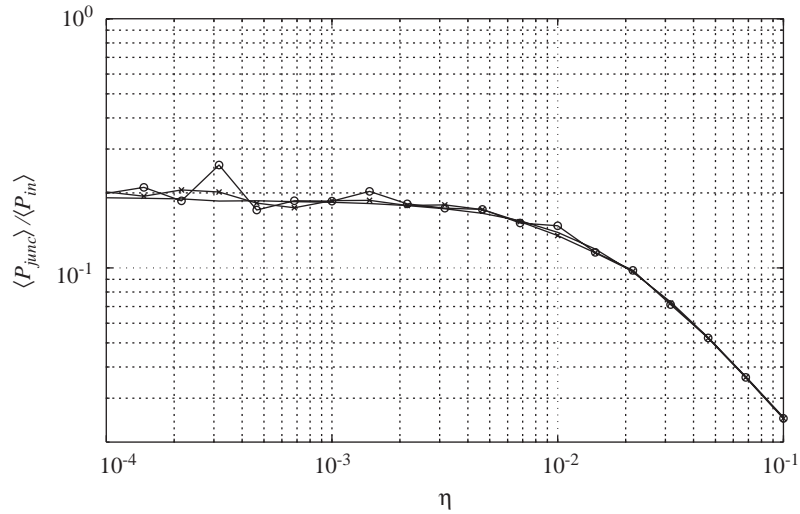


Fig. 12. Ensemble-averaged junction power as a function of the loss factor η for the *regular* system, by numerical averaging over the Monte Carlo ensemble (—), from a single scalar ensemble average (—o—o—) and from the average of 10 scalar ensemble averages (—x—x—).

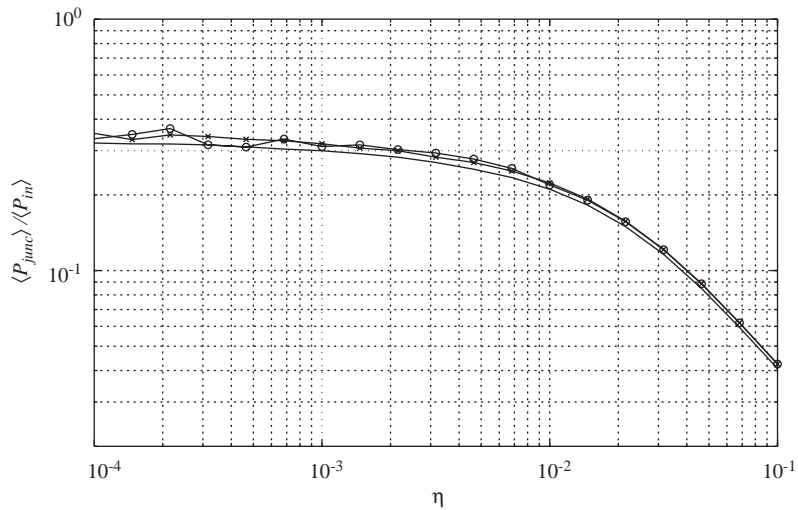


Fig. 13. Ensemble-averaged junction power as a function of the loss factor η for the *irregular* system, by numerical averaging over the Monte Carlo ensemble (—), from a single scalar ensemble average (—o—o—) and from the average of 10 scalar ensemble averages (—x—x—).

5.3. Variances

Corresponding estimates of the variance of the junction power are shown in Figs. 14 and 15. Both of these figures show that considerably fewer samples are required by the scalar ensemble

approach to produce variance estimates of comparable accuracy; even a single estimate provided by the scalar ensemble method gives reasonable accuracy. It should be noted, however, that the computational cost involved in evaluating the variance over the scalar ensemble can be significant for structures involving many wave components. For structures involving n wave components, evaluation of expressions involving products of matrices of order $n^2 \times n^2$ is required.

6. Concluding remarks

In this paper, a number of observations made in a companion paper concerning the relevance of the scalar ensemble to practical ensembles of structures have been demonstrated quantitatively for example ensembles of regular and irregular two-plate structures. In particular, a key assumption of the scalar ensemble approach concerning the close association between ensemble variations in energy response and variations in the common phase of the eigenvalues of the matrix product \mathbf{ST} has been demonstrated for the example ensembles. The probability distribution of junction powers over the scalar ensemble has been shown to be a good approximation to the distribution obtained by Monte Carlo simulation for each of the examples structures examined.

The accuracy of analytical expressions for mean and variance of response, also derived in a companion paper, has been verified for the example structures. The better accuracy achieved in the case of the irregular structure is consistent with the expected effects of stronger eigenvalue repulsion in these structures.

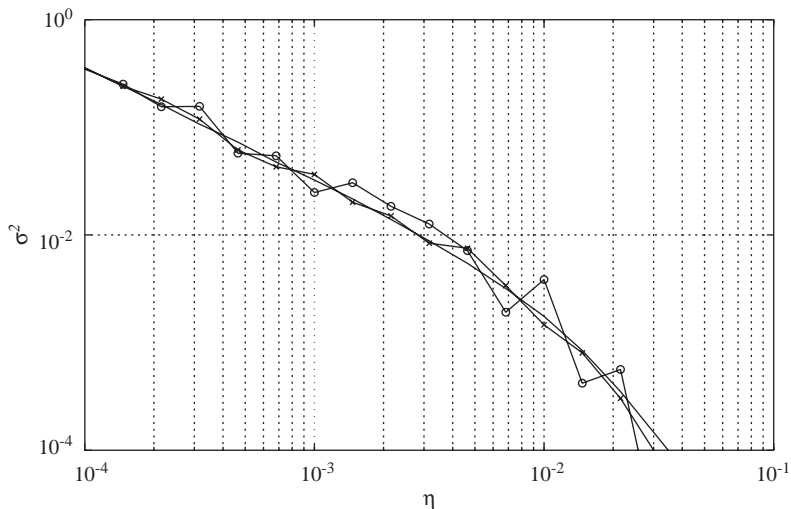


Fig. 14. Variance of normalised junction power as a function of the loss factor η for the *regular* system, by numerical method over the Monte Carlo ensemble (—), from a single scalar ensemble variance estimate (—o—o—) and from the average of 10 scalar ensemble variance estimates (—x—x—).

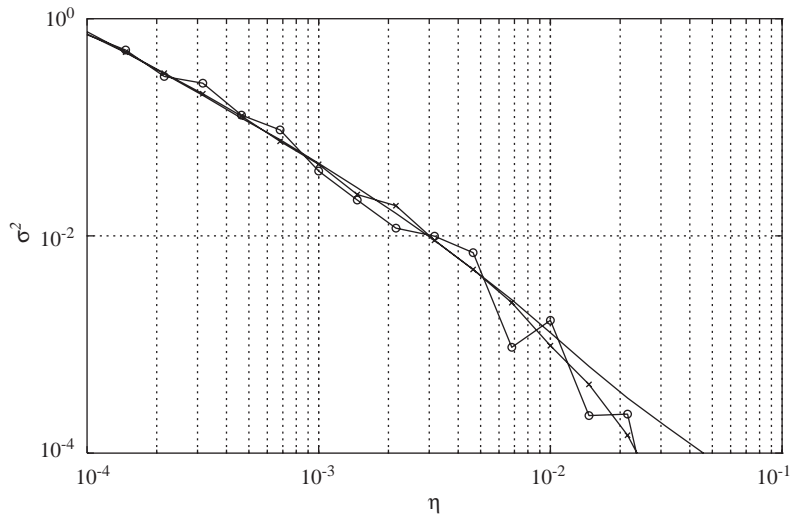


Fig. 15. Variance of normalised junction power as a function of the loss factor η for the *irregular* system, by numerical method over the Monte Carlo ensemble (—), from a single scalar ensemble variance estimate (—o—o—) and from the average of 10 scalar ensemble variance estimates (—x—x—).

References

- [1] R.H. Lyon, R.G. DeJong, *Theory and application of Statistical Energy Analysis*, second ed., Butterworth-Heinemann, Boston, 1995.
- [2] E.C.N. Wester, B.R. Mace, Wave component analysis of energy flow in complex structures – Part I: a deterministic model, *Journal of Sound and Vibration* 285 (2005) 209–227, this issue.
- [3] E.C.N. Wester, B.R. Mace, Wave component analysis of energy flow in complex structures – Part II: ensemble statistics, *Journal of Sound and Vibration* 285 (2005) 251–265, this issue.
- [4] E.C.N. Wester, B.R. Mace, Statistical energy analysis of two edged-coupled rectangular plates: ensemble averages, *Journal of Sound and Vibration* 193 (1996) 793–822.
- [5] E.C.N. Wester, A wave component approach to the analysis of vibrations in complex structures, *Ph.D. Thesis*, University of Auckland, New Zealand.
- [6] B.R. Mace, J. Rosenberg, The SEA of two coupled plates: an investigation into the effects of subsystem irregularity, *Journal of Sound and Vibration* 212 (1998) 395–415.